Available online at www.sciencedirect.com
ScienceDirect
Journal of Power Sources 173 (2007) 695–699
JOURNAL OF POWER SOURCES
www.elsevier.com/locate/jpowsour

Short communication

Structural and electrical properties of selected $La_{1-x}Sr_xCo_{0.2}Fe_{0.8}O_3$ and $La_{0.6}Sr_{0.4}Co_{0.2}Fe_{0.6}Ni_{0.2}O_3$ perovskite type oxides

Konrad Świerczek [a,*], Makoto Gozu [b]

[a] *Faculty of Materials Science and Ceramics, AGH University of Science and Technology, al. Mickiewicza 30, 30-059 Kraków, Poland*
[b] *Faculty of Engineering, Shibaura Institute of Technology, 3-7-5 Toyosu, Koto-ku, Tokyo 135-8548, Japan*

Available online 21 May 2007

Abstract

In this paper, the structural and transport properties of selected $La_{1-x}Sr_xCo_{0.2}Fe_{0.8}O_3$ (LSCF) perovskites and $La_{0.6}Sr_{0.4}Co_{0.2}Fe_{0.6}Ni_{0.2}O_3$ (LSCFN64262) perovskite are presented. Crystal structure of the samples was characterized by means of X-ray studies with Rietveld method analysis. DC electrical conductivity and thermoelectric power were measured at a wide temperature range (80–1200 K) in air. For $La_{0.2}Sr_{0.8}Co_{0.2}Fe_{0.8}O_3$ (LSCF2828) and $La_{0.4}Sr_{0.6}Co_{0.2}Fe_{0.8}O_3$ (LSCF4628) perovskites a maximum observed on electrical conductivity dependence on temperature exists at about 750 K. It can be associated with an appearance of oxygen vacancies and implies a mixed ionic-electronic transport. A growing amount of oxygen vacancies at higher temperatures causes a decrease in the electrical conductivity due to a recombination mechanism associated with lowering of the average valence of 3d metals. A similar characteristic was found for LSCFN64262 perovskite, which also exhibits a relatively high electrical conductivity.

Keywords: LSCF; LSCFN; Solid Oxide Fuel Cell (SOFC); Transport properties; Thermoelectric power

1. Introduction

Lowering of the working temperature of Solid Oxide Fuel Cells is crucial for the further development of the SOFC technology [1,2]. However, at an intermediate temperature range (870–1070 K) several serious drawbacks appear. At these temperatures solid electrolytes show the insufficiently high ionic conductivity (a greater IR drop of the cell). Also, a deterioration of the transport and catalytic properties of electrode materials occurs. In order to obtain satisfying power outputs of SOFC within this range of temperatures it is necessary to optimize all the elements of the cell. In case of electrolytes it is accomplished either by using the ones with a higher ionic conductivity or/and by minimizing the thickness of the electrolyte layer [3,4]. For the cathode materials one of the most important aspects is the occurrence of the mixed ionic-electronic conductivity. This, in turn, allows for the oxygen reduction on active centres on the entire surface of cathode material (not only on triple phase boundary) and the oxygen ion transport in whole cathode bulk [5]. The mixed ionic-electronic conductivity can be achieved by an appropriate chemical composition of the cathode material [6,7]. However, all other essential properties of the material, especially a high catalytic activity towards oxygen reduction and fitting thermomechanical properties towards the electrolyte must be maintained.

Among other materials, LSCF perovskites seem to be particularly interesting in terms of their possible application and have been extensively studied as potential cathode materials [8–10]. It was possible to reach over 550 mW cm^{-2} at 870 K with a composite, 50:50 wt.% LSCF8228–$Ce_{0.9}Gd_{0.1}O_{1.95}$ cathode and 10 μm thick $Ce_{0.8}Gd_{0.2}O_{1.9}$ electrolyte [11]. Recently, $Ba_{0.5}Sr_{0.5}Co_{0.8}Fe_{0.2}O_3$ (BSCF) and $Sm_{0.6}Sr_{0.4}CoO_3$ (SSC) perovskites were also successfully applied in intermediate temperature SOFCs. The obtained power outputs at 870 K exceeded 1300 mW cm^{-2} for cell with 10 μm thick $Gd_{0.1}Ce_{0.9}O_{1.95}$ electrolyte and BSCF cathode material [12] and over 1900 mW cm^{-2} for cell with SSC cathode material fabricated on the surface of 5 μm LSGM electrolyte with 400 nm thick SDC buffer layer [13].

In this work, we report a study of selected $La_{1-x}Sr_xCo_{0.2}Fe_{0.8}O_3$ (LSCF) perovskites and $La_{0.6}Sr_{0.4}Co_{0.2}Fe_{0.6}Ni_{0.2}O_3$ (LSCFN64262) perovskite from synthesis and structural characterization to transport properties at high and low temperatures.

* Corresponding author. Tel.: +48 12 6172026; fax: +48 12 6172026.
E-mail address: xi@agh.edu.pl (K. Świerczek).

0378-7753/$ – see front matter © 2007 Elsevier B.V. All rights reserved.
doi:10.1016/j.jpowsour.2007.05.052

Table 1
Structural properties of LSCF and $La_{0.6}Sr_{0.4}Co_{0.2}Fe_{0.6}Ni_{0.2}O_3$ perovskites

Composition	Space group	*a* [Å]	*b* [Å]	*c* [Å]	Cell volume [Å]^3
$LaCo_{0.2}Fe_{0.8}O_3$	*Pnma* (62)	5.5116 (2)	7.7995 (3)	5.5331 (2)	237.86 (2)
$La_{0.8}Sr_{0.2}Co_{0.2}Fe_{0.8}O_3$[a]	*R*-3*c* (167)	5.5226 (3)	–	13.3894 (8)	353.65 (3)
$La_{0.6}Sr_{0.4}Co_{0.2}Fe_{0.8}O_3$[a]	*R*-3*c* (167)	5.5010 (1)	–	13.3754 (4)	350.53 (1)
$La_{0.4}Sr_{0.6}Co_{0.2}Fe_{0.8}O_3$	*Pm*-3*m* (221)	3.8670 (1)	–	–	57.83 (1)
$La_{0.2}Sr_{0.8}Co_{0.2}Fe_{0.8}O_3$	*Pm*-3*m* (221)	3.8640 (1)	–	–	57.69 (1)
$La_{0.6}Sr_{0.4}Co_{0.2}Fe_{0.6}Ni_{0.2}O_3$[a]	*R*-3*c* (167)	5.4727 (1)	–	13.2462 (3)	343.58 (1)

[a] Lattice parameters presented in hexagonal symmetry.

2. Experimental

$LaCo_{0.2}Fe_{0.8}O_3$ and $La_{0.8}Sr_{0.2}Co_{0.2}Fe_{0.8}O_3$ perovskites were synthesized using precursors obtained by a citric acid method. Synthesis details are presented elsewhere [14]. For other samples, instead of citric acid, the ammonia salt of EDTA (ethylenediaminetetraacetic acid) was used as a complexing agent. The obtained precursors were initially heated in air for 1 h at 1270 K, milled using zirconia balls and pressed uniaxially into pellets (100 MPa). The final heating was performed in air at 1470 K for 24 h with slow cooling to RT. We were unable to synthesize single phase $SrCo_{0.2}Fe_{0.8}O_3$ sample following this procedure, similar difficulties were reported before [15]. Crystal structure of the samples was characterized by the XRD studies using Phillips X'Pert Pro difractometer. Goldschmidt's tolerance factor *t* [16] was calculated using ionic radii presented by Shannon [17], taking into account an existence of mixed valence in 3d metal sublattice. The X-ray patterns were analyzed using Rietveld method with RayFlex software. DC electrical conductivity was measured by a four-probe method in 300–1200 K temperature range in air and by a pseudo four-probe method in 80–300 K range. Thermoelectric power (TEP) measurements were carried out at 80–1200 K temperature range by means of a dynamic method with a variable temperature gradient. TEP of gold electrodes was taken into account in calculation of TEP of the samples.

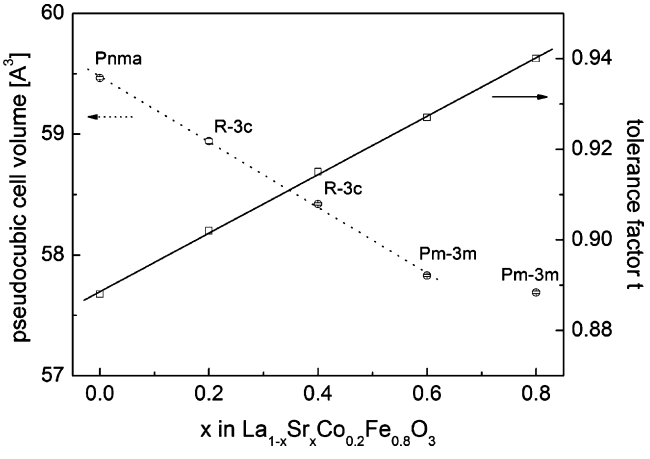

Fig. 1. Pseudo-cubic cell volume and tolerance parameter *t* as a function of strontium amount in LSCF perovskites.

3. Results and discussion

The structural data obtained at room temperature (RT) by a refinement of the X-ray diffraction patterns of selected LSCF perovskites and LSCFN64262 compound are presented in Table 1. All samples were found to be single phase. These materials possess different crystal structures at RT, depending on lanthanum and strontium amount. The data for LSCF compounds presented in Fig. 1 are shown as dependence between the pseudo-cubic cell volume (e.g. volume of the cubic unit

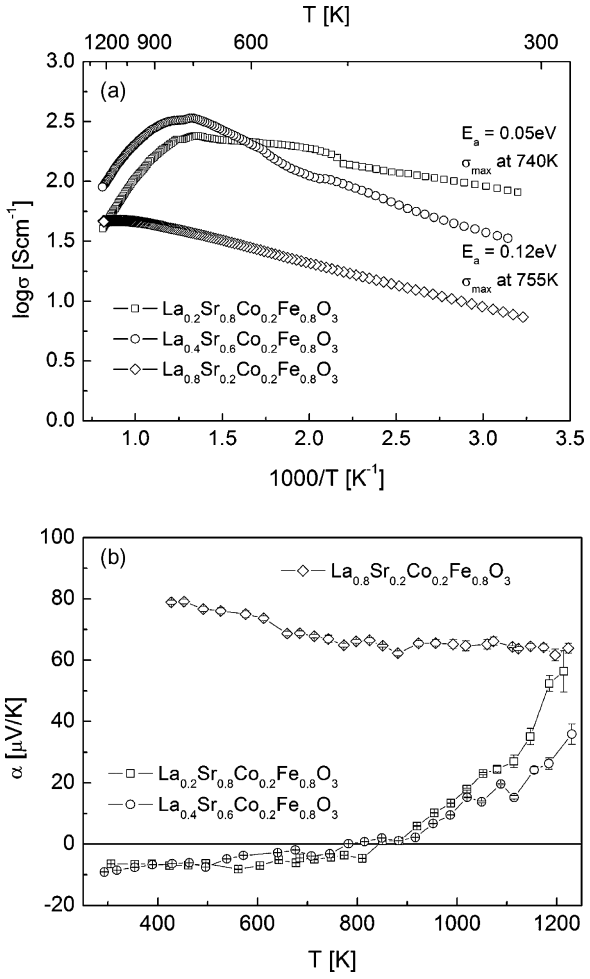

Fig. 2. (a) Electrical conductivity and (b) thermoelectric power of $La_{0.4}Sr_{0.6}Co_{0.2}Fe_{0.8}O_3$, $La_{0.2}Sr_{0.8}Co_{0.2}Fe_{0.8}O_3$ and $La_{0.8}Sr_{0.2}Co_{0.2}Fe_{0.8}O_3$ perovskites at high temperatures.

cell, which in case of *Pnma* or *R*-3*c* structure is distorted) and the amount of strontium. The volume of the cell decreases with an increasing strontium content in a linear way, except for LSCF2828 sample. A different behaviour of LSCF2828 sample is probably due to an oxygen nonstoichiometry at RT, which is higher than in LSCF4628 composition. As the LSCF structure evolves on doping towards a cubic one, a tolerance factor *t* increases correspondingly, which is a typical behaviour [18]. The LSCFN64262 sample possesses a *R*-3*c* structure at RT, similarly to other LSCFN compounds [19]. Substitution of 0.2 mol of iron by nickel in this compound (in relation to LSCF6428) is accompanied by a significant decrease of the unit cell parameters (Table 1).

High temperature electrical conductivity data for selected LSCF compounds are presented in Fig. 2a. The results of TEP measurements for LSCF perovskites at 300–1200 K range are shown in Fig. 2b. A clearly visible maximum in electrical conductivity dependence on temperature is visible for both LSCF4628 and LSCF2828 perovskites and occurs at 755 K for LSCF4628 and at 740 K for LSCF2828. These maxima can be related to the beginning of formation of oxygen vacancies in the perovskite structure according to an equation:

$$O_O \leftrightarrow V_O^{\bullet\bullet} + 2e^- + 0.5O_2 \uparrow . \quad (1)$$

One may expect that electrons created in this process should increase electrical conductivity, however, the results are opposite. Such behaviour may be explained by the recombination reaction, in which a high valence 3d metal (Co^{4+}, Fe^{4+}) is reduced to a lower (3+) valence. As the ionic conductivity is overshadowed by an electronic component [20], despite the presence of mobile oxygen vacancies in the perovskite structure, it is safe to assume that the vacancies do not affect total conductivity. The observed electrical conductivity drops are significant, nevertheless, the total conductivity of the samples remains high. Thermoelectric power results at high temperatures follow corresponding electrical conductivity changes. Initially, TEP sign is negative for both LSCF4628 and LSCF2828 (contrary to LSCF8228), suggesting dominance of electrons as charge carriers (Fig. 2b). Experiential values of TEP for LSCF4628 and LSCF2828 are quite small and do not change up to about 700–750 K. It is worth noting, that for both samples TEP starts to change at about the same temperature, in which the maximum of electrical conductivity is observed (Fig. 2a). At higher

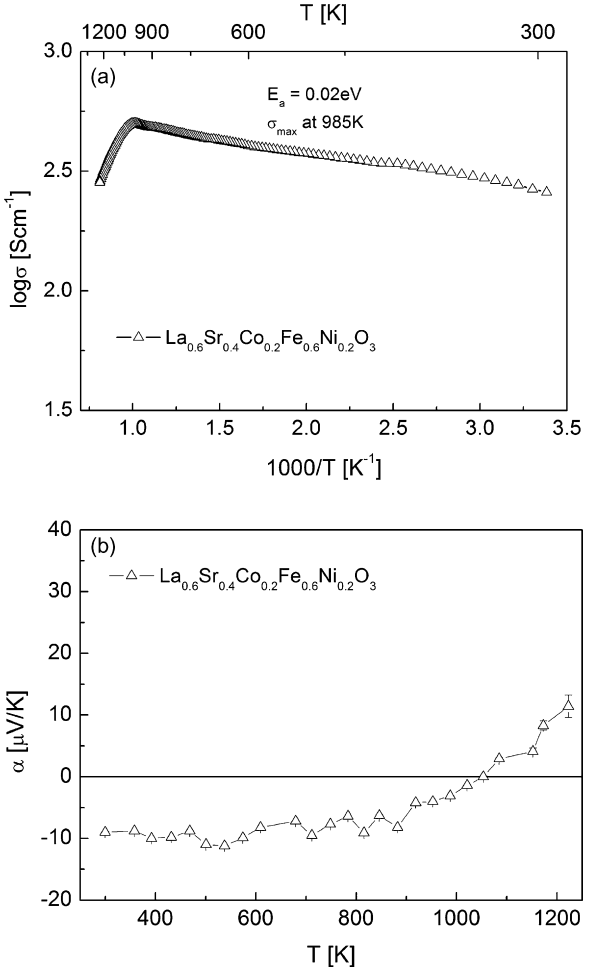

Fig. 3. (a) Electrical conductivity and (b) thermoelectric power of $La_{0.6}Sr_{0.4}Co_{0.2}Fe_{0.6}Ni_{0.2}O_3$ at high temperatures.

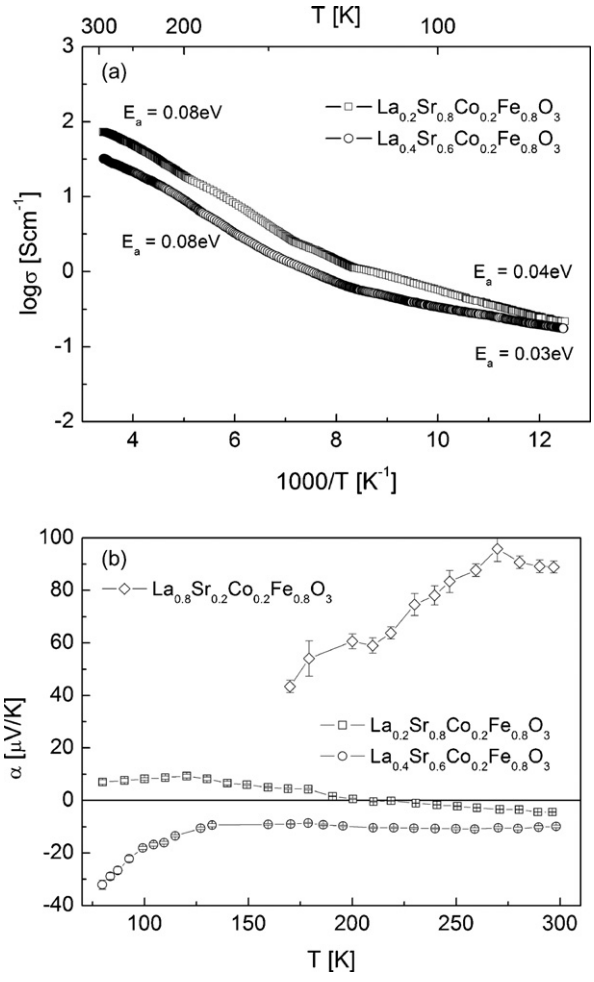

Fig. 4. (a) Electrical conductivity and (b) thermoelectric power of $La_{0.4}Sr_{0.6}Co_{0.2}Fe_{0.8}O_3$, $La_{0.2}Sr_{0.8}Co_{0.2}Fe_{0.8}O_3$ and $La_{0.8}Sr_{0.2}Co_{0.2}Fe_{0.8}O_3$ perovskites at low temperatures.

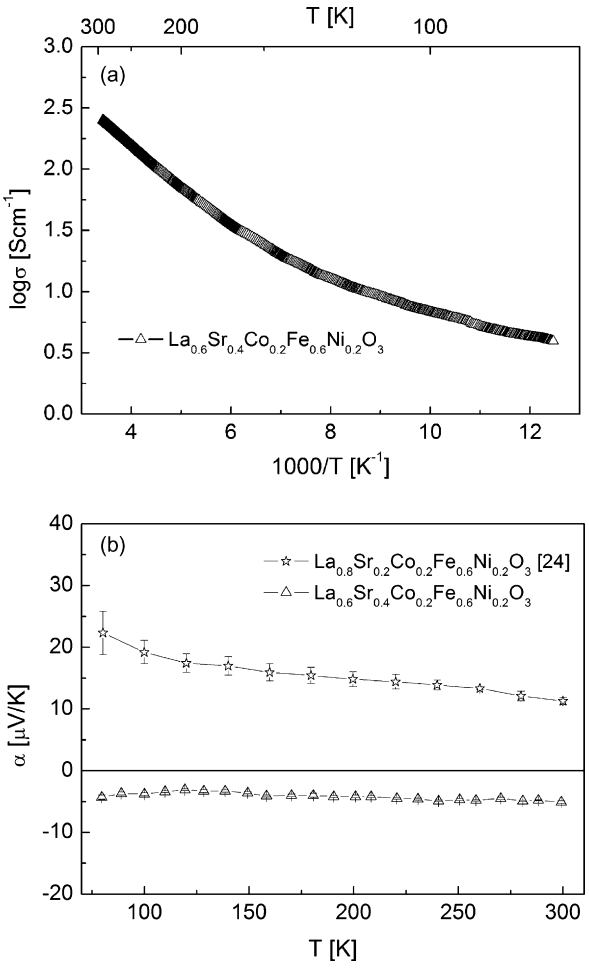

Fig. 5. (a) Electrical conductivity and (b) thermoelectric power of $La_{0.6}Sr_{0.4}Co_{0.2}Fe_{0.6}Ni_{0.2}O_3$ at low temperatures. Data for LSCFN82262 taken from [24].

temperatures a quite rapid increase of TEP is recorded and the sign of thermoelectric power changes from a negative to a positive one, being directly connected to an increase of oxygen nonstoichiometry in the perovskite structure. For higher level of Sr doping a conduction band in LSCF is filled only partially, giving *n* type of conduction. As temperature increases, the level of nonstoichiometry increases and electrons created in this process (Eq. (1)) fill the conduction band. Consequently, a *p* type of conduction is observed. Similar TEP values of LSCF4628 and LSCF2828 perovskites probably originate from different initial level of oxygen deficiency. The previous report by Stevenson et al. indicated that oxygen vacancy concentration δ, which lowers the average oxidation state of 3d metals, equals to about 0.01 for LSCF4628. However, for LSCF2828 composition δ is about 0.04 [7].

In Fig. 3a and b high temperature measurements of transport properties of LSCFN64262 sample are presented. A maximum of electrical conductivity for this sample appears at 985 K, which is about 250 K higher comparing to LSCF4628 or LSCF2828. This sample, however, demonstrates higher values of electrical conductivity, reaching 500 S cm^{-1} at 985 K, than LSCF perovskites. Also the activation energy of electrical conductivity of this sample is the lowest one and equals to 0.02 eV. Thermoelectric power of LSCFN64262, similarly to LSCF samples, is negative and nearly constant, but around 900 K begins to increase and above 1000 K sign of TEP changes to positive one (Fig. 3b). This phenomenon may be also related, likewise in case of LSCF, to the increase of oxygen nonstoichiometry of the sample.

Low temperature transport properties of selected LSCF materials are presented in Fig. 4a and b. It should be emphasized that both samples differ in their oxygen stoichiometry, as it was presented above. Electrical conductivity of LSCF4628 and LSCF2828 perovskites is very similar at low temperature range (Fig. 4a) and is considered to occur due to the polaron hopping mechanism [7,21]. TEP values are also similar, but below 130 K thermoelectric power of LSCF4628 decreases while for LSCF2828 sample it changes sign to a positive one around 200 K and slightly increases, reaching maximum around 120 K. This behaviour can be related to a different shape of $dN(\varepsilon)/d\varepsilon$ at the Fermi level. Similar, complicated temperature dependence of TEP at low temperature range was found for LSF and other perovskites [22,23].

Electrical conductivity of LSCFN64262 perovskite at low temperature range is presented in Fig. 5a. A non-Arrhenius characteristic is observed with high values (4 S cm^{-1} at 80 K). Thermoelectric power data of LSCFN64262 sample is shown in Fig. 5b. TEP at measured temperature range is negative and nearly temperature independent.

4. Conclusions

LSCF4628, LSCF2828 and LSCFN64262 perovskites synthesized using precursors obtained by the soft chemistry EDTA method were found to possess attractive transport properties in 870–1070 K range. This favours their possible application in the intermediate temperature SOFCs. Oxygen nonstoichiometry, which appears at high temperatures leads to the mixed ionic-electronic transport, indispensable for the cathode materials.

Acknowledgement

This work is supported by Polish Committee for Scientific Research under grant PBZ-100/1/3/2004.

References

[1] N.Q. Minh, J. Am. Ceram. Soc. 76 (1993) 563–588.
[2] A. Boudghene Stambouli, E. Traversa, Renew. Sust. Energy Rev. 6 (2002) 433–455.
[3] V. Thangadurai, W. Weppner, Ionics 12 (2006) 81–92.
[4] X. Chen, N.J. Wu, L. Smith, A. Ignatiev, Appl. Phys. Lett. 84 (2004) 2700–2702.
[5] S.B. Adler, J.A. Lane, B.C.H. Steele, J. Electrochem. Soc. 143 (1996) 3554–3564.
[6] S.J. Skinner, Int. J. Inorg. Mater. 3 (2001) 113–121.
[7] J.W. Stevenson, T.R. Armstrong, R.D. Carneim, L.R. Pederson, W.J. Weber, J. Electrochem. Soc. 143 (1996) 2722–2729.
[8] A. Esquirol, N.P. Brandon, J.A. Kilner, M. Mogensen, J. Electrochem. Soc. 151 (2004) A1847–A1855.
[9] A. Petric, P. Huang, F. Tietz, Solid State Ionics 135 (2000) 719–725.

[10] E. Maguire, B. Gharbage, F.M.B. Marques, J.A. Labrincha, Solid State Ionics 127 (2000) 329–335.
[11] Y.J. Leng, S.H. Chan, S.P. Jiang, K.A. Khor, Solid State Ionics 170 (2004) 9–15.
[12] Q.L. Liu, K.A. Khor, S.H. Chan, J. Power Sources 161 (2006) 123–128.
[13] J. Yan, H. Matsumoto, M. Enoki, T. Ishihara, Electrochem. Solid State Lett. 8 (2005) A389–A391.
[14] K. Świerczek, J. Marzec, D. Pałubiak, W. Zając, J. Molenda, Solid State Ionics 177 (2006) 1811–1817.
[15] J.-H. Wan, J.-Q. Yan, J.B. Goodenough, J. Electrochem. Soc. 152 (2005) A1511–A1515.
[16] V.M. Goldschmidt, Naturwissenschaften 14 (1926) 477–485.
[17] R.D. Shannon, Acta Cryst. A32 (1976) 751–767.
[18] M. Imada, A. Fujimori, Y. Tokura, Rev. Mod. Phys. 70 (1998) 1039–1263.
[19] K. Świerczek, J. Marzec, J. Molenda, Mater. Sci.-Poland 24 (2006) 115–122.
[20] Y. Teraoka, H.M. Zhang, K. Okamoto, N. Yamazoe, Mater. Res. Bull. 23 (1988) 51–58.
[21] L.-W. Tai, M.M. Nasrallah, H.U. Anderson, D.M. Sparlin, S.R. Sehlin, Solid State Ionics 76 (1995) 273–283.
[22] K. Huang, H.Y. Lee, J.B. Goodenough, J. Electrochem. Soc. 145 (1998) 3220–3227.
[23] H.D. Zhou, J.B. Goodenough, J. Solid State Chem. 178 (2005) 3679–3685.
[24] K. Świerczek, J. Marzec, W. Ojczyk, J. Molenda, Defect Diffusion Forum 237–240 (2005) 1293–1298.